URTeC: 2455932

Development of Limited Discrete Fracture Network using Surface Microseismic Event Detection Testing in Canadian Horn River Basin

*Claudio Virues, Jason Hendrick, Nexen Energy ULC; Sudhendu Kashikar, Microseimic Inc.

This paper was prepared for presentation at the Unconventional Resources Technology Conference held in San Antonio, Texas, USA, 1-3 August 2016.

Summary

In 2010 a noise test and microseismic emission detection test was performed in the Horn River Basin in northeastern British Columbia, Canada, to determine a) the suitability for surface microseismic monitoring and b) the character of the near-surface noise in an effort to determine the optimal depth to bury geophones.

The test consisted of a low density, low aperture array of 14 stations that covered the heels of eight wells. Initially the array was used to capture six treatments located outside of the array footprint. Two additional stages, located under the array footprint, were recorded and processed at a later date.

This coarse array allowed for the detection of several hundred events and a single moment tensor solution was determined. A dip-slip focal mechanism with a failure plane oriented NE-SW. This information, however not ideal, was adequate to create a limited amplitude based discrete fracture network (DFN) to be developed for the test results as well as a preliminary estimate of stimulated reservoir volume (SRV) for the test stages. Microseismic events that were imaged that were located outside of the array had larger positional uncertainty and reduced amplitudes compared to events recorded from stages within the array. This was a limitation imposed by the aperture of the array used in the test, as well as the low number of stations.

Test results indicate that the Horn River Basin is an adequate environment for surface microseismic monitoring, with good signal-to-noise characteristics. The test results suggest that adequate surface noise suppression is achieved by placing the sensors at or below 30m depth. The test also demonstrates that there is a need for appropriate array fold and wider aperture in order to fully describe the fracture network and obtain the most reliable estimates of SRV.

Introduction

In 2010, a permanent shallow buried array consisting of 14 stations was deployed over an area of 2.5km x 2.3km on the Dilly Creek property in the Horn River Basin in northeast British Columbia, Canada (Figure 1). A buried array design was chosen based on a number of factors including; the long well lengths, which reached 2500m of lateral length, changing completions schedules and timing, and difficulties with event multipathing which can complicate downhole processing (Eisner, 2009). The array was designed to monitor 32 hours of completions activities on an 8-well pad. The limited monitoring time was due to the high monitoring and processing costs, and the noise test objective was met with 32 hours of recording.

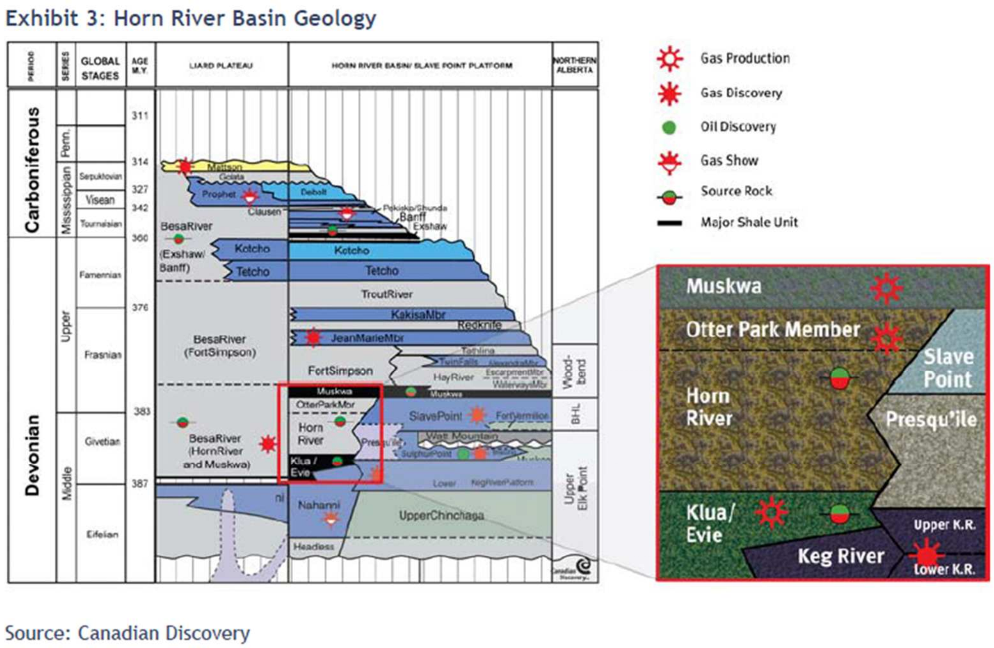

Figure 1: Horn River Basin Stratigraphic Correlation Chart

Surface microseismic survey design

The goals of using microseismic monitoring include: visualizing and evaluating the stimulated reservoir volume (SRV), well and stage spacing, completions techniques and ultimately to recommend changes to the well design to maximize future resource recovery. To accomplish this, a large high density network of surface stations is required, at a high cost. To ensure this array would be effective, a small test array at the well pad 1 was installed. This array tested design parameters that included sensor depths, noise levels and event location effectiveness. The test array was designed using single level three-component 10 Hz sondes to image hydraulic fracture stimulations in the Muskwa, Otter Park and Evie formations in the mid Devonian at approximately 2500 m below the array. The number of stations used was selected to ensure that signal could be separated from background noise.

Thirteen stations had a single geophone cemented between 50 and 75 m depths. The 14th station contained a five-level array consisting of one and three component sensors, drilled to a depth of 100 m. Each station was supplemented with 1C surface geophone arrays. Sensors were modeled and placed in an ideal network over the pad. The array aperture was designed such that the distance from the edge of the array to the nearest well is approximately the target depth, which in this case was between 2300 and 2500 m. The array aperture was designed to capture wide-azimuth, full-fold data and maintain consistent microseismic mapping over the entire pad (Zhang, 2011). Stations were repositioned to accommodate geological, environmental and cultural features. At Dilly Creek, the stations were moved to avoid changes in shallow subsurface geology, facilities and roads. Existing seismic cut-lines were utilized in the design to increase ease of station access and minimize environmental disturbance. Since this was the operator's first surface array in the area, 14 sensors were used to over-sample the data to ensure a high signal to noise ratio during recording. Sampling was at 1 millisecond and was set for continuous recording. The final design is shown in Figure 2. The sensors were oriented with hammer shot locations near the stations from known locations.

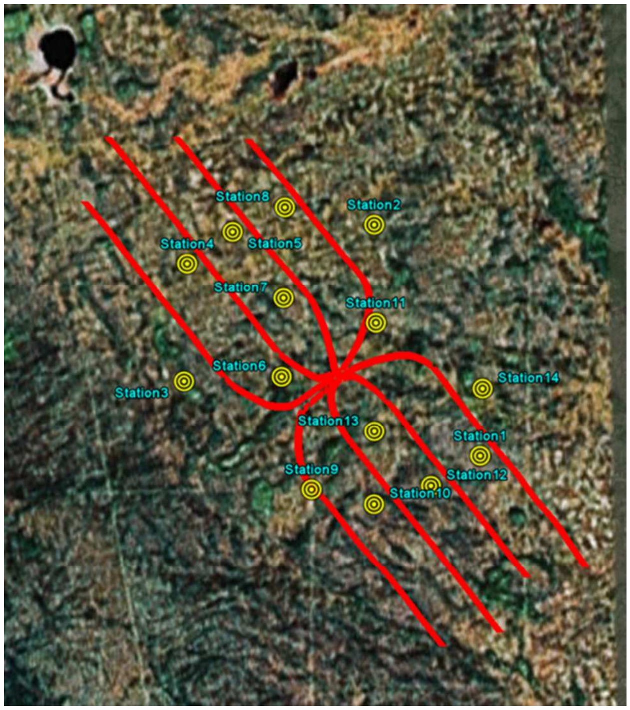

Figure 2: Event detection test on an 8 well pad

Data Collection

Each site was connected to a laptop and the data was manually downloaded. Access to surface points was very limited due to the summer muskeg ground conditions. Access at the remote sites was only possible by tracked Argo all-terrain vehicle (see Figure 3: Manual Data Collection). Each site was connected to a PC and the data was manually downloaded. The download time was a function of the amount of accumulated data. Manual data collection for the scale of this project was more cost effective than a telemetric data collection system.

Figure 3: Manual Data Collection: Tracked Argo

Processing

While in the Field, preliminary data preparation and transcription was done. A first dataset of 6 frac treatment stages was sent to the vendor for the noise and detectability testing. An additional dataset was later sent for moment tensor analysis. The velocity for the imaging was estimated at 4,200 meters/second and a constant velocity was used. A 1D model was used to create a 3D volume encompassing the area of interest. The Velocity volume bins were 20 meters in X, Y and Z.

Noise was a concern at this location and a consideration for station depth. Surface facilities, including a camp, are located within the array as well as heavily used roads. In addition to surface noise, shallow quaternary channels from 50-200 m depth were noted to degrade the signal quality on 3D seismic gathers, and were a concern for surface microseismic signal quality. In the final design, some stations are relocated to avoid these channels.

Noise and Event Detection Test

The test was conducted in July/August 2010 during the hydraulic fracturing completions program at an 8 well pad. By placing sensors at various depths and recording during treatment, noise attenuation with depth can be quantified and the optimal burial depth identified. This is recommended when installing monitoring arrays in new exploration areas or areas with unknown near surface attenuation levels. It was found that a sufficient reduction in noise was obtained at 30 m burial with marginal additional noise reduction at 100 m depth. The Quaternary channels underlying the array also placed a constraint on sonde depth since these could be gas-charged and pose a drilling hazard. It was deemed that the optimal depth for balancing noise suppression and drilling costs was 30 m for the entire array.

Data Quality – Background noise levels by depth (Figure 4 **and** Figure 5**)**

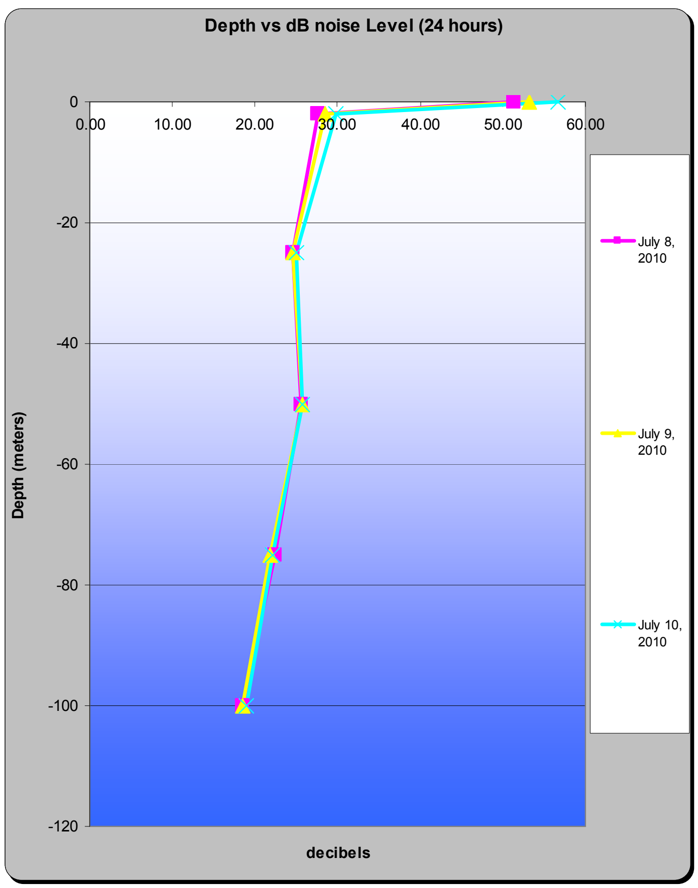

Figure 4: Background noise levels by depth (24 hours)

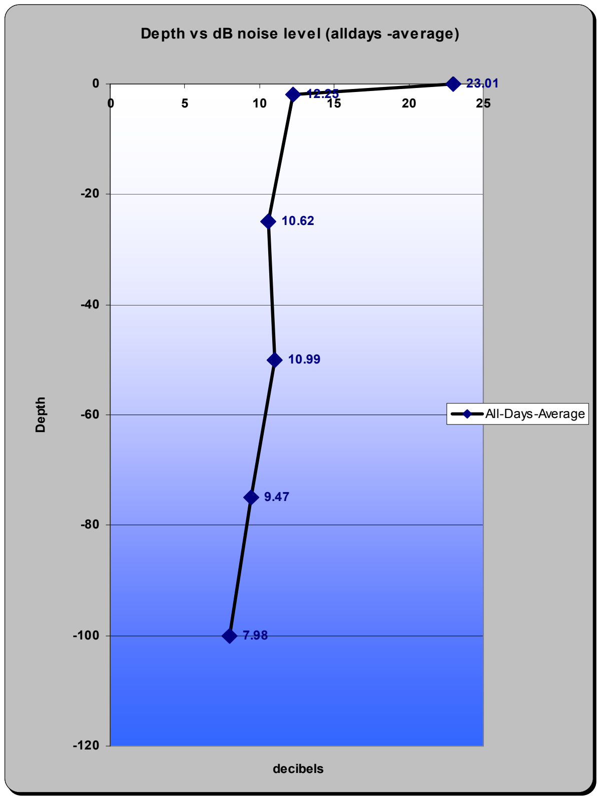

Figure 5: Background noise levels by depth (all days - average)

Initially six fracture treatments were recorded on July 8 thru 10th, 2010 (see Figure 6). Two additional stages were recorded on July 27th thru August 1st, 2010 (see Figure 7)

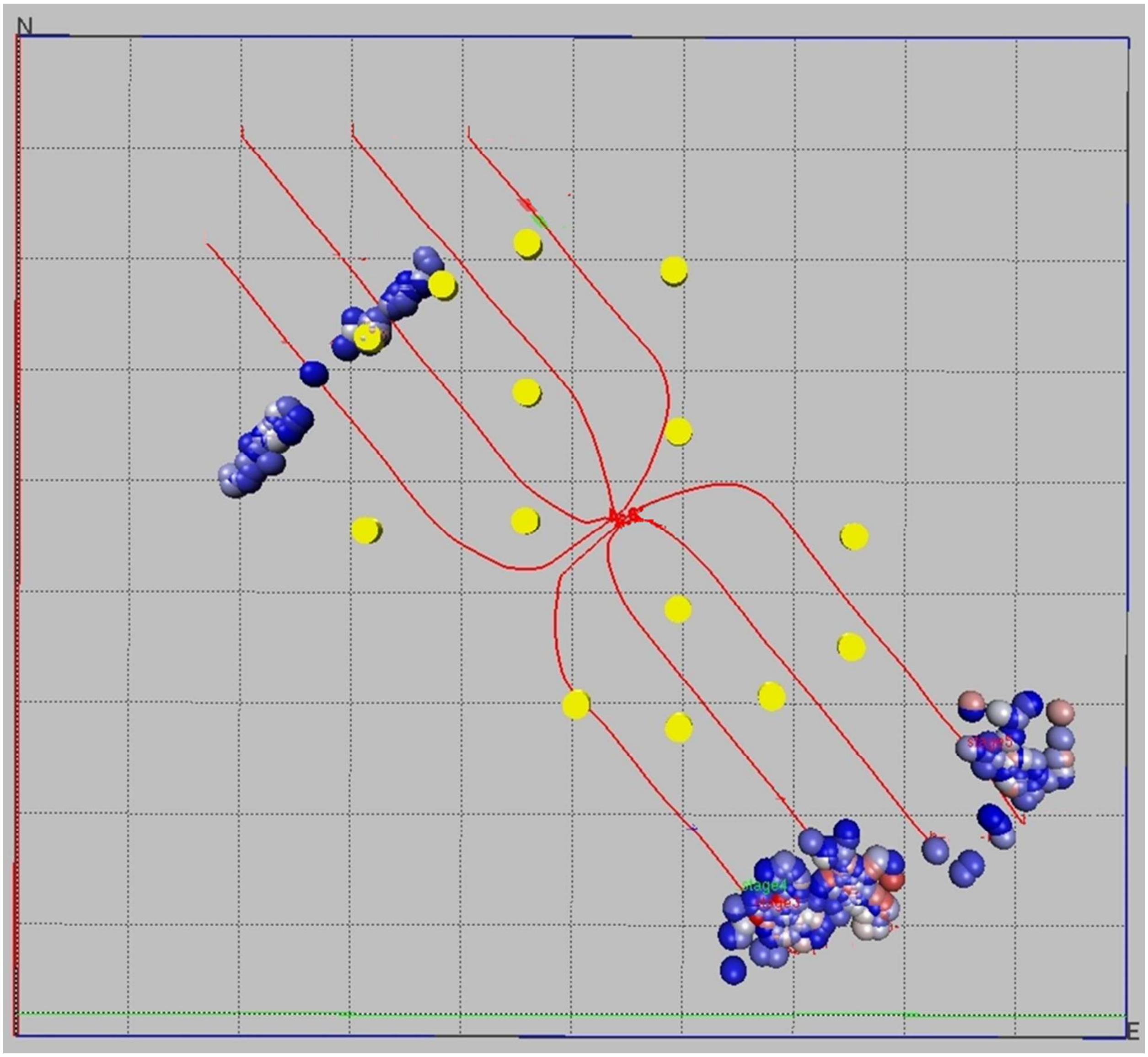

Figure 6: Detected microseismic events during recording window (first dataset)

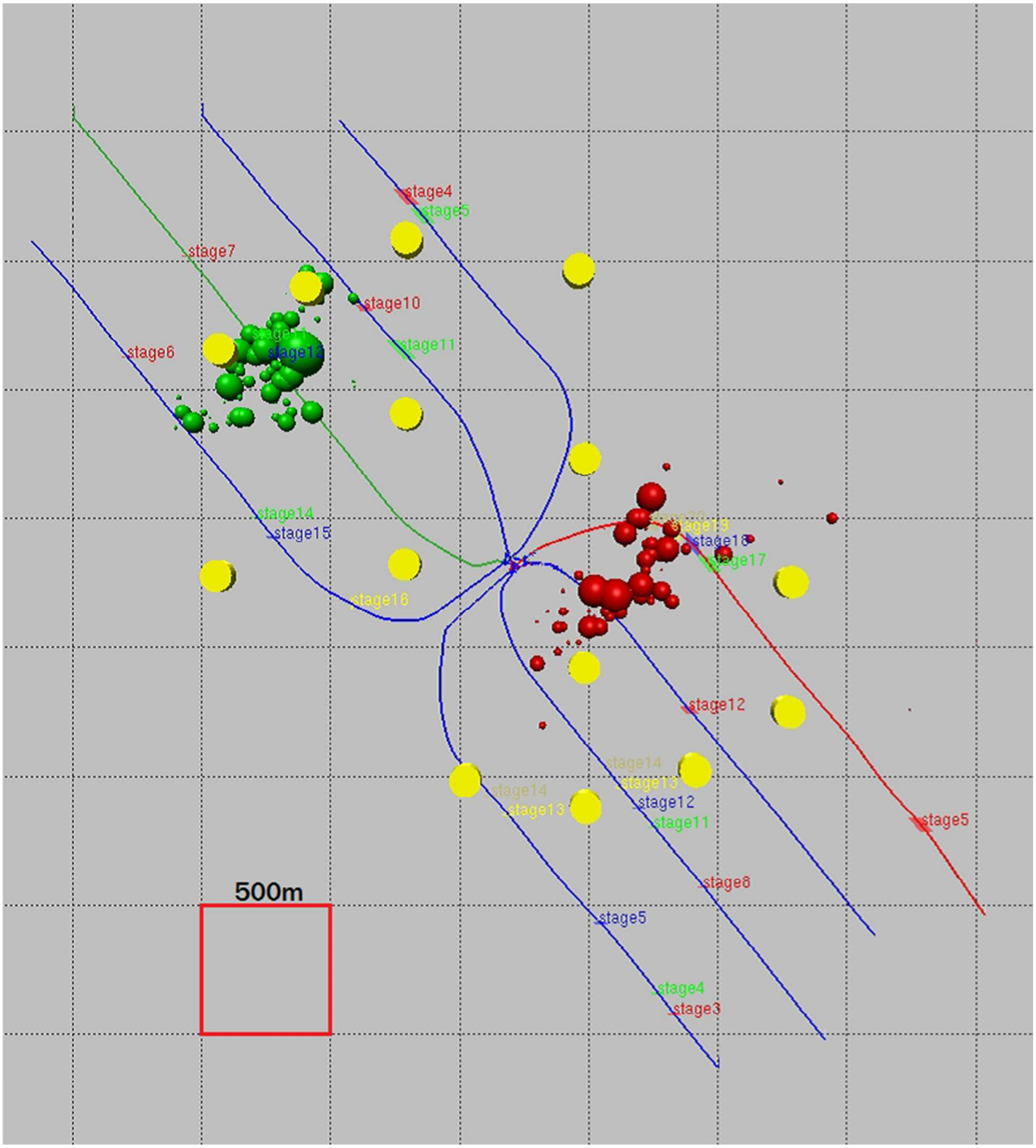

Figure 7 : Subsequent Recording (July 27-August 1, 2010)

Figure 8 and Figure 9 show the second data set for moment tensor analysis.

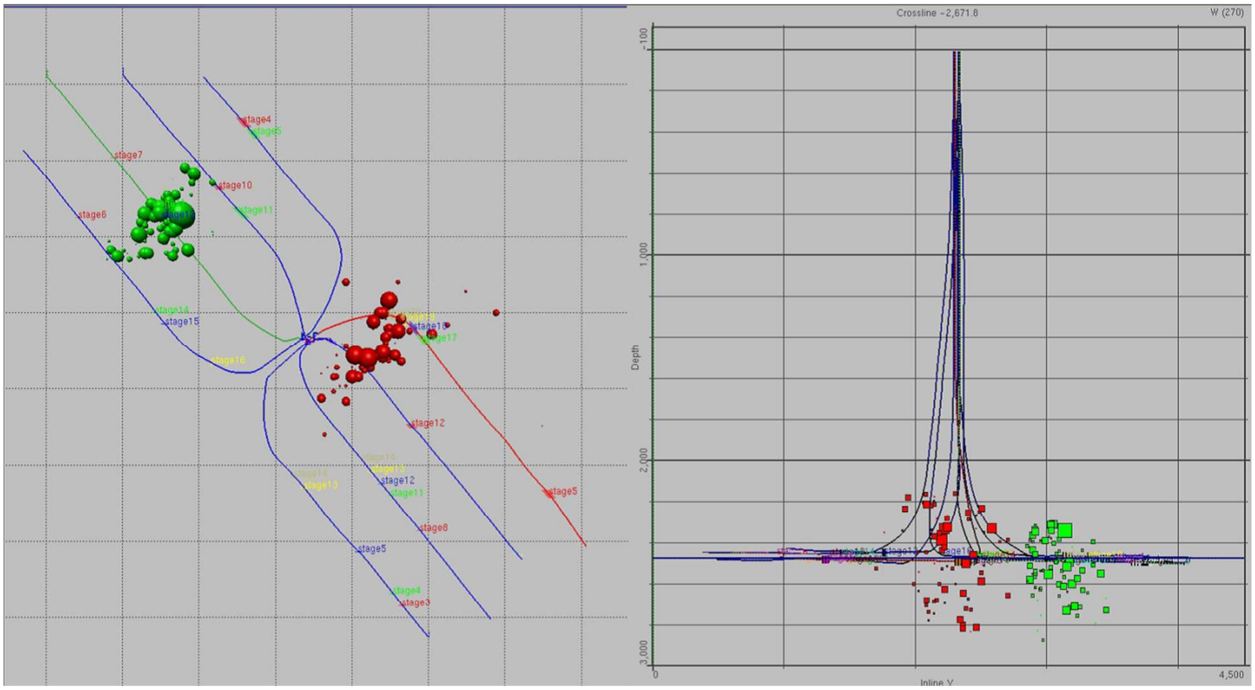

Figure 8: Map View and Depth View (second dataset for moment tensor analysis)

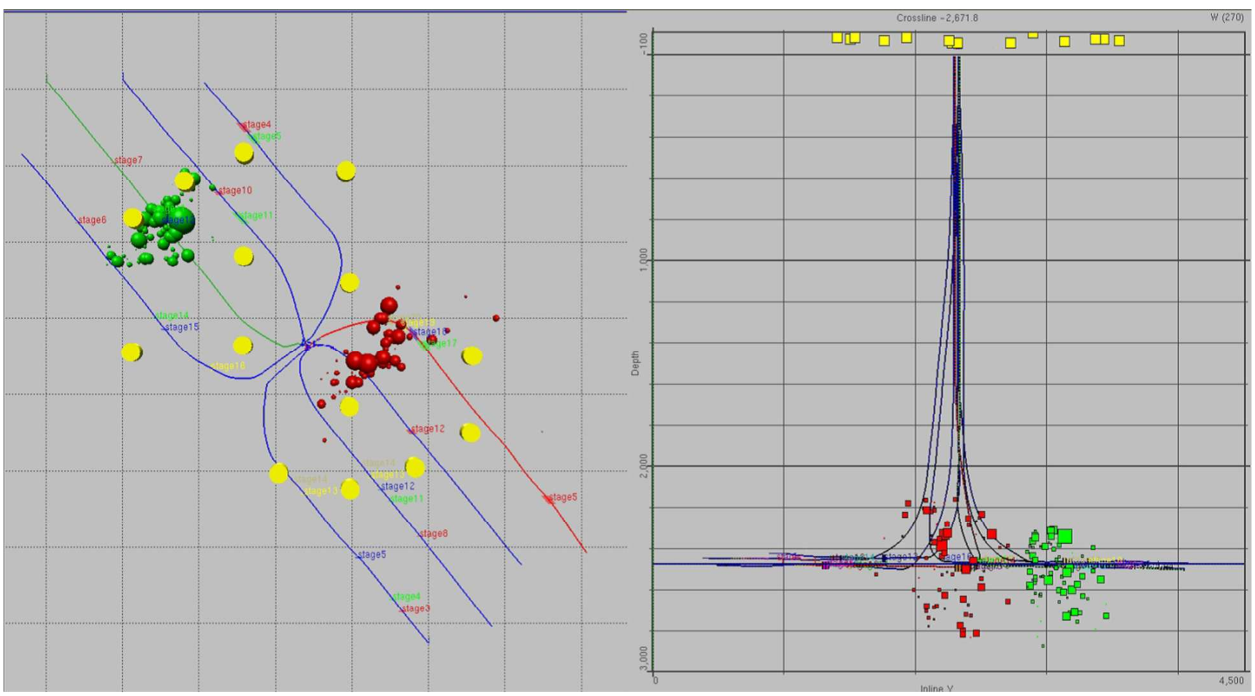

Figure 9: Map View and Depth View (second dataset for moment tensor analysis)

Focal Mechanism

Since the noise-event detection test was a sparse array, only one event detected could be inverted for a focal mechanism. The event was a dip-slip event (see Figure 10). This is a constrained solution, which means only the double-couple solution is considered. The test did not have enough sampling to obtain full moment tensor information with high confidence. Moment tensor is typically obtained with an array that monitors most of the focal sphere around a microseismic emission. This is due to better sampling better and provides a higher confidence solution. Moment tensor solutions generally require multiple borehole arrays that are not coplanar with the event to obtain the proper six independent components to obtain full resolution as described by Baig and Urbancic (2010).

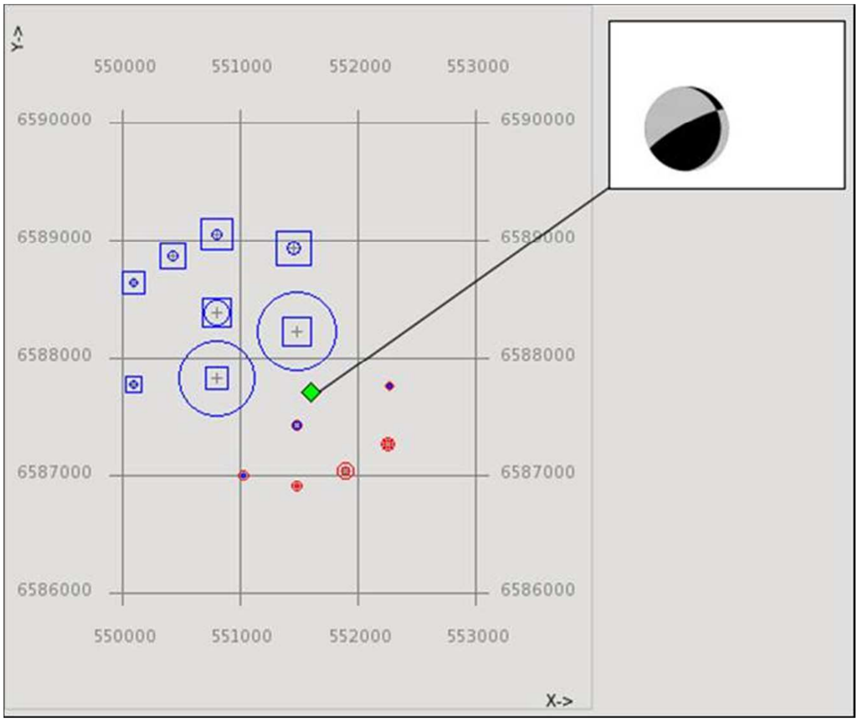

Figure 10

Figure 10: Focal Mechanism Solution (negative polarity in blue, positive polarity in red)

Designing the DFN

In Figure 11 points located from both recording periods (initial and subsequent) are used to construct a Discrete Fracture Network model (DFN).

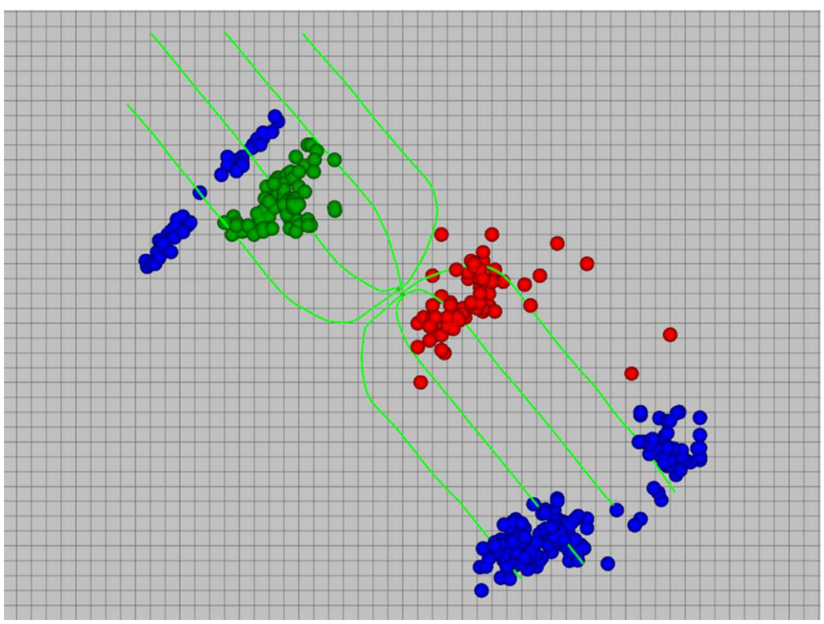

Figure 11: 8 Well pad with points used to construct a DFN model

Magnitude Calibrated Discrete Fracture Network

A magnitude-based calibrated Discrete Fracture Network (DFN) methodology based on microseismicity induced during stimulation of a wellbore has been developed that incorporates magnitude of the event and associated microseismic moment (M)), rock rigidity (μ), injected fluid volumes (Vi), and fluid efficiency (η). Fundamentally, for every microseismic hypocentre, fracture area (A) = M/μδ .

The seismic moment (M0), which is defined as Aμδ (A is area of the slip plane, μ is shear modulus, and δ is average displacement along the slip plane), is a fundamental equation that relates seismic source parameters to actual measured variables (Kanamori, 1977). μ is obtained from sonic logs. Displacement is initially estimated as a function of M_o by assuming a constant stress drop of 3 MPa using data by Bohnhoff et al. (2010).

Assuming an aspect ratio that reflects the overall geometry of the microseismic cloud (e.g. for an aspect ratio of 0.5, fracture height, h, is 0.5L where L is the length of the fracture) the geometry of each fracture with a hypocenter seismic moment (M0) can be calculated.

This implies that the fractures were centered on event locations and fracture sizes were based on the amplitude / magnitude of the events. Fracture size ranged from 30-120 m, with Strike 45 degrees and Dip of 90 degrees as determined through the focal mechanism.

Figure 12 shows a map view of the deterministic fractures on a grid 100 m*100 m*100 m.

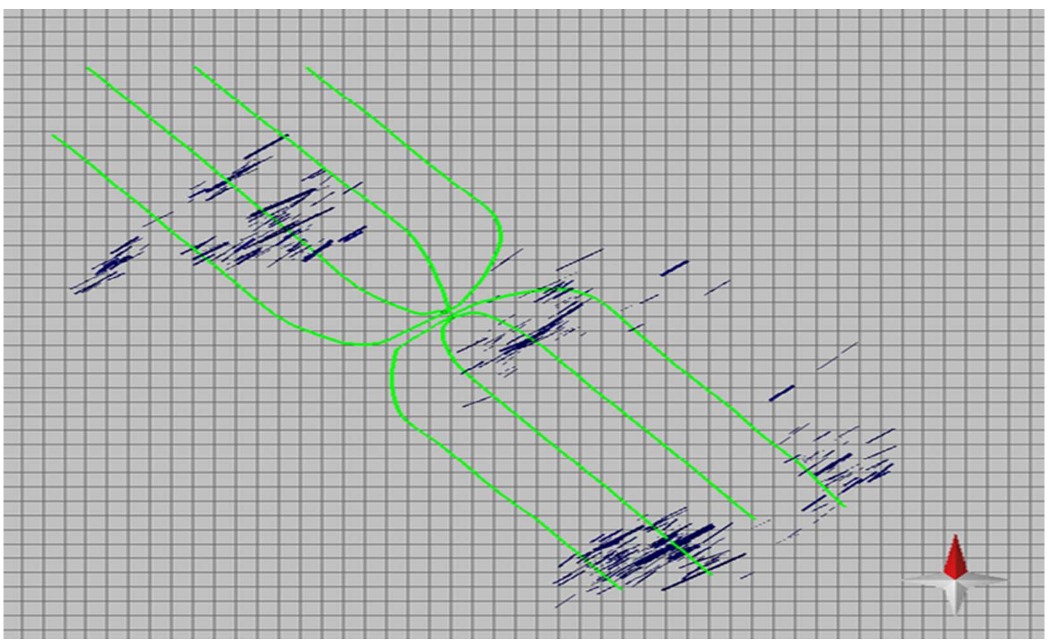

Figure 12: Deterministic fractures on a grid 100 m * 100 m* 100 m (strike 45 degrees, dip 90 degrees) – Map View

Fracture Aperture

McGarr (1976) related total detected seismicity to injected volumes assuming that the change in volume is completely accommodated by the seismic failure using the equation $\Sigma M0 = k\mu|\Delta Vi|$ where k is a scaling factor ranging from 0 to 1 which could account for fluid leaking off into the formation. This leakoff volume can be determined from a Diagnostic Fracture Injection Test (DFIT). Total fracture volume, $Vf = A\Delta u$. A is the surface area of the fracture, Δu is the opening of the fracture that is empirically related to the length of the fracture using a power law relation (e.g. Vermilye and Scholz, 1995), height of the fracture is related to the length by the aspect ratio defined above. Thus the aperture is defined as proportional to root length of individual fractures.

$\Delta u = 0.001c\sqrt{l}$, where Δu is the aperture, c is a coefficient and l is the length of the fracture. Typically a coefficient c of 0.55 will yield an average aperture of 3.0 mm.

Stimulated Rock Volume

In order to calculate the total Stimulated Rock Volume (SRV), a three-dimensional grid is applied to the total DFN. Every grid-cell containing a non-zero fracture property is included in the SRV. The total SRV is dependent on the size of the model cells and can be adjusted based on known reservoir flow properties. It represents the total rock volume that was affected by the treatment.

In this paper, the model shows one possible fracture configuration. Fracture size in the DFN has been based on locally calibrated event magnitudes. The fracture orientations are defined by regional information, focal mechanism and the event trend azimuth, with a statistical scatter applied. The model could be calibrated with rock properties data and production data in a later phase.

Figure 13 shows an oblique view of the geocellular Stimulated Rock Volume for the stages where microseismic data was acquired.

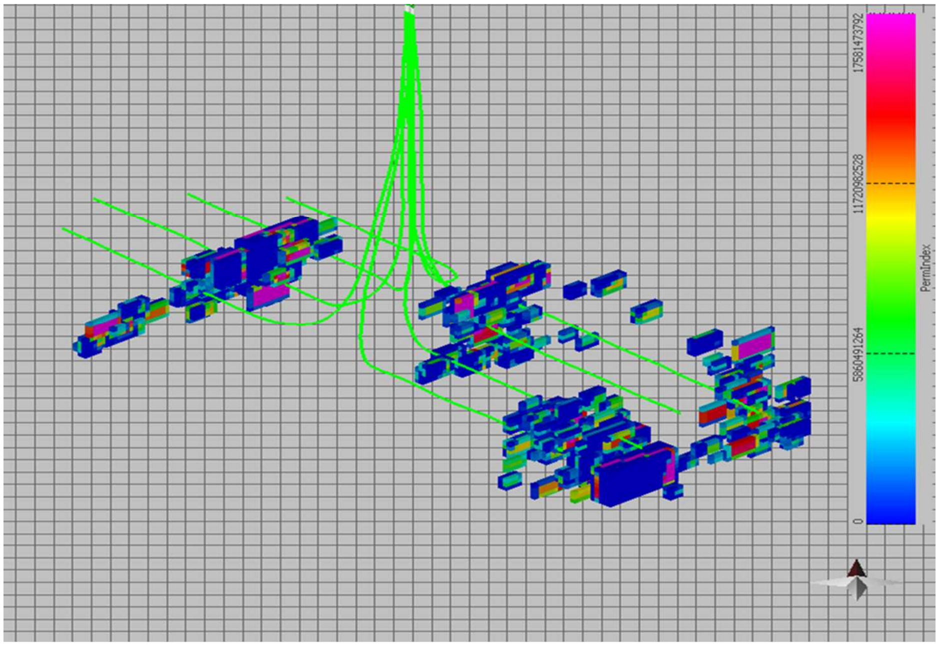

Figure 13: Geocellular Stimulated Rock Volume - Oblique View

Calculated Output Fracture Flow Properties

Here we leverage work done by Oda on quantifying permeability for a fractured reservoir. The technique is used to compute a permeability tensor in a geocell (volume of rock) containing fractures. Long et al. (1982) has suggested that a rock mass behaves more like a porous medium if a sufficient number of discontinuities (i.e. fractures) are present. Thus if we have a knowledge of the fracture intensity (number of fractures, orientation of fractures and aperture of fractures) we can compute a permeability tensor that describes the effective permeability for the cell in X, Y and Z directions (see Figure 14). The DFN and SRV workflow described above provide us with a description and quantification of the fracture intensity within each geocell. We can compute the number of fractures, the orientation of individual fractures as well as aperture of individual fractures contained within the geocell. Applying the Oda technique yields a permeability tensor for each geocell. By applying the same equation for permeability computation in every geocell, the relative magnitude of the permeability accurately describes the fluid flow through the system.

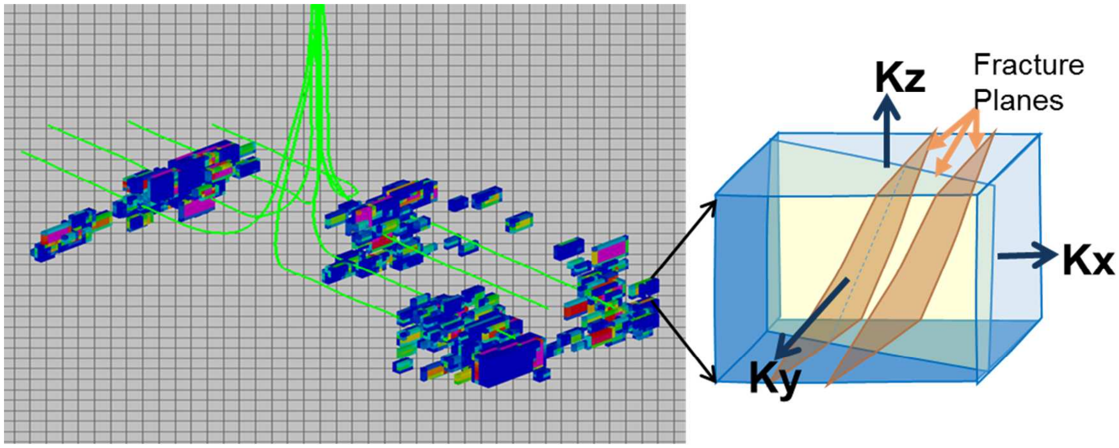

Figure 14: Effective Permeability Tensor Computation from DFN model for Individual Geocell

A permeability index is then computed that retains the scaling of the permeability between individual cells rather than the absolute permeability value as computed by the Oda methodology. The absolute permeability will be determined through production history matching or other techniques.

The geocellular volume shows the distribution of the effective permeability enhancement generated through hydraulic fracturing from the discrete fracture network. Note the higher permeabilities in the zones of dense microseismicity.

Figure 15 shows the effective permeability model in plan view with cells of 30 m * 30 m * 30 m. Figure 16 thru Figure 18 show fracture permeability models for different TVDs. Hot colors indicate high permeability.

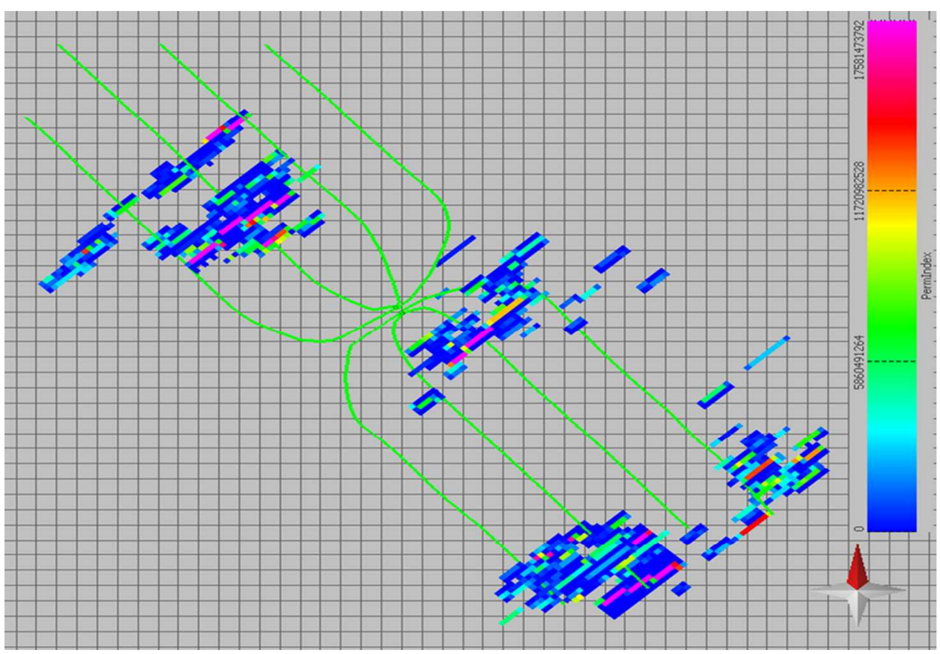

Figure 15: Effective Permeability Model – Plan View (Cells 30*30*30 m, Grid 100*100*100 m)

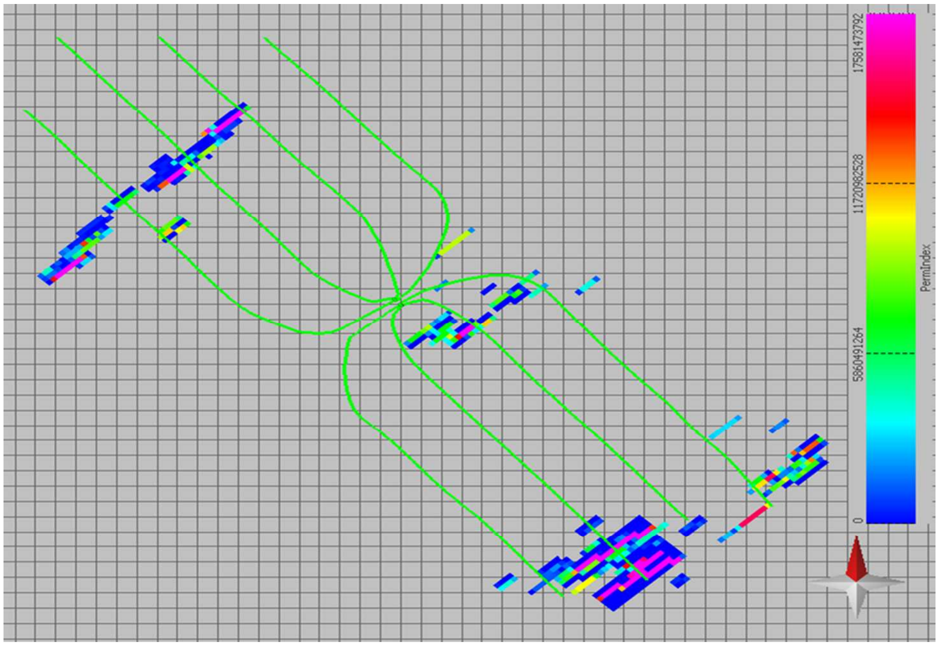

Figure 16: Effective Permeability Model – Plan View @ 200m TVD above the wellbore (Cells 30*30*30 m, Grid 100*100*100 m)

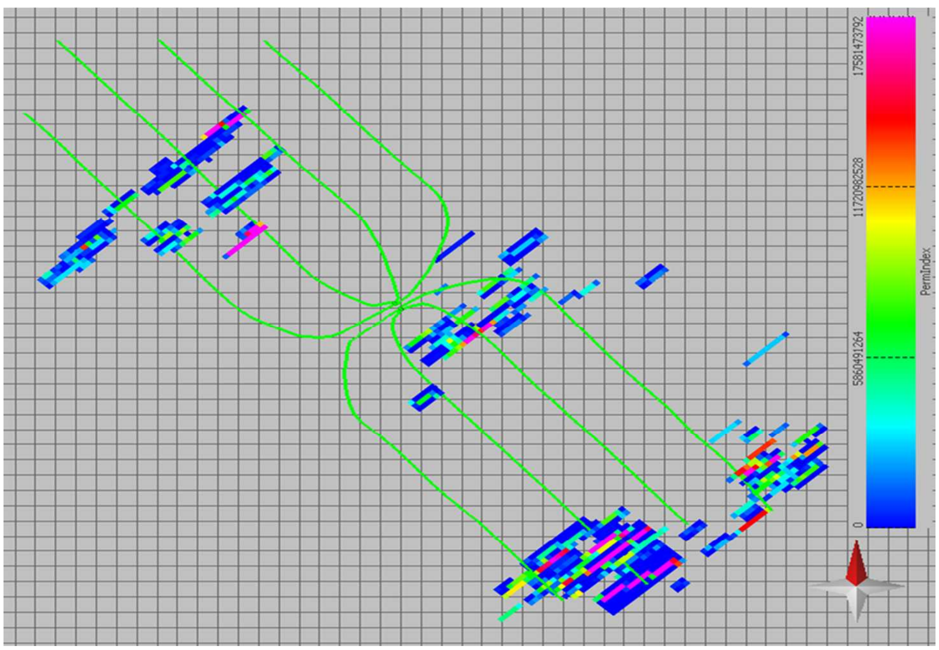

Figure 17: Effective Permeability Model – Plan View @ Wellbore TVD (Cells 30*30*30 m, Grid 100*100*100 m)

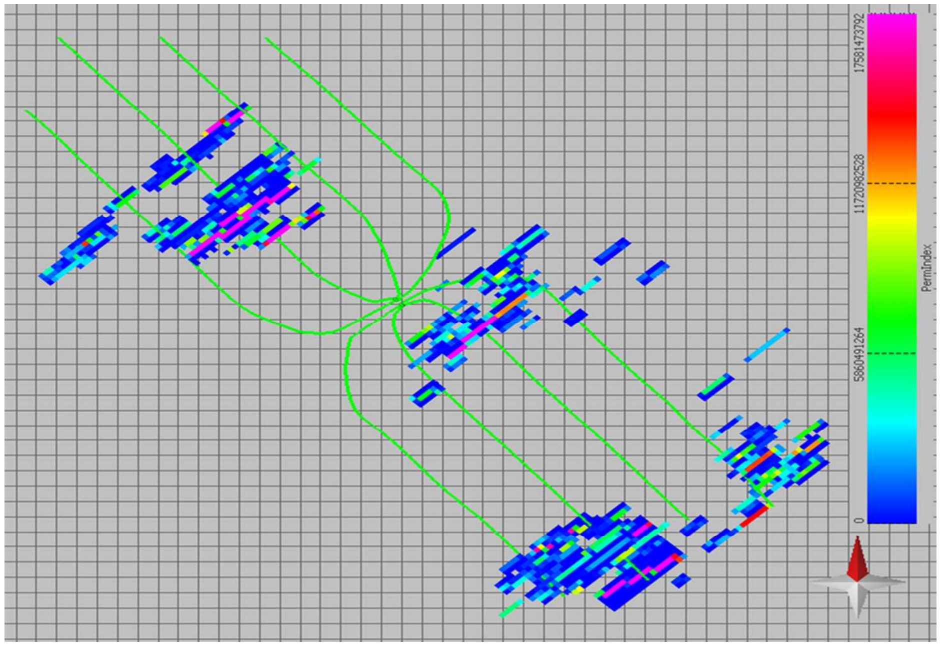

Figure 18: Fracture Permeability Model – Plan View @ 200m TVD BELOW the wellbore(Cells 30*30*30 m, Grid 100*100*100 m)

Geocellular Volume-based SRV Calculation

The effective permeability model allows a visualization of an SRV calculated from a DFN. Every cell containing a non-zero fracture flow property is included in the stimulated volume total. The volume of cells containing fracture flow properties are summed to obtain a total SRV for the treatment well. The total SRV volume is dependent on the size of the model cells, and can be adjusted based on known reservoir flow properties.

Results and Discussion

Results from the Noise Test

The noise test shows a correlation to noise reduction with depth. A 20 dB noise reduction is seen in the near subsurface. The average dB down from the surface was 25dB. Once the sensors are placed below the muskeg layer in the first 0-20 meters, the noise decrease rate flattens as shown in Figure 4 and 5. The noise level decreases at a lower rate as the depth approaches the deepest sensor at 100m. Additional channels helps to stack out noise and increased the detectability of microseismic events. The sensors placed at the deepest depth had the lowest noise level therefore increased the detectability. Several hundred microseismic events were detected on the array over the short monitoring periods. The microseismic events exhibited both P and S waves during times of hydraulic fracturing, with lower frequencies than recorded borehole microseismic events. One focal mechanism solution was determined and compared to borehole microseismic results. Factors such as sensor coupling and drill type will also be considered in selecting optimal depths for future stations. Casing perforation shot times for 5 completion stages were given to the vendor, one shot was detected on the surface array for a frac stage, and used for time synchronization.

Results from the DFN

Average Fracture Aperture	**0.004 m**
Average Fracture Porosity	**7.2e-08 (unitless)**
Total Fracture Surface Area	**673,336 m^2**
Total Fracture Volume	**1457.89 m^3**
Stimulated Rock Volume	**43,036,364 m^3**

Total Fracture Surface Area is the double of the sum of fracture half-length multiplied by fracture height.
Total Fracture Volume is the sum of fracture void space in the volume, calculated from fracture areas and apertures.
Stimulated Rock Volume is the volume of geocellular cubes that have fracture properties (the affected rock matrix).

Conclusions

A noise test was successfully performed using the sparse surface array. Valuable information was gleaned that will help to plan future larger scale surface microseismic monitoring arrays. Information about noise levels, sensor and station placement, data downloading and transmission, attenuation and hodogram resolution was obtained. A DFN has been created using the noise detection test data. Considerations for event placement accurately and certainty must be considered in the future. The perforation shot calibration helps to constrain the uncertainty in event location, as well as improving the velocity model. Microseismic monitoring projects recently have improved the understanding of the velocity field. They have revealed a complex anisotropic velocity field that greatly affects the event locations. This may influence final DFN values such as Stimulated Reservoir Volume, fracture area and fracture volume. Results from DFN modeling are meant for demonstration purposes only, however it was demonstrated that a DFN could be successfully created using sparse data from a noise test on a small surface array.

References

Aki, K., Richards, P.G., 1980. Quantitative Seismology, Freeman and Co., New York

Detring, J., & Williams-Stroud, S. (2012). *Using Microseismicity to Understand Subsurface Fracture Systems and Increase the Effectiveness of Completions:* Eagle Ford Shale, TX. Society of Petroleum Engineers.

Baig, A., T. Urbancic, 2010, Microseismic moment tensors: A path to understanding frac growth: The Leading Edge, March 2010, 320-324, doi/pdf/10.1190/1.3353729

Bulant, P., L. Eisner, I. Psencik, and J. L. Calvez, 2007, Importance of borehole deviation surveys for monitoring of hydraulic fracturing treatments: Geophysical Prospecting, **55**, no. 6, 891–899, doi:10.1111/j.1365-478.2007.00654.x.

Chambers, K., S. Brandsberg-Dahl, J.-M. Kendall, and J. Rueda, 2008, Testing the ability of surface arrays to locate microseismicity: 78th Annual International Meeting, SEG, Expanded Abstracts, 1436–1440.

Duncan, P. and L. Eisner, (2010): Reservoir characterization using surface microseismic monitoring. *Geophysics*, 75**,** No. 5**,** pp. 75A139–75A146; doi:10.1190/1.3467760.

Duncan, P. M., J. D. Lakings, and R. A. Flores, 2010, Method for passive seismic emission tomography: U. S. Patent 7,663,970 B2.

Eisner, L., W., P. M. Duncan, M. Heigl, and W. R. Keller, 2009, Uncertainties in passive seismic monitoring: The Leading Edge, **28**, 648–655, doi:10.1190/1.3148403.

Eisner, L, B. J. Hulsey, P. Duncan, D. Jurick, H. Werner, W. Keller. 2010: Comparison of surface and borehole locations of induced microseismicity. *Geophysical Prospecting*, doi: 10.1111/j.1365-2478.2010.00867.x

Heidbach, O. Tingay, M, Barth, A., Reinecker, J., Kurfeβ, D., and Müller, B., 2008: The 2008 release of the World Stress Map <available online at www.world-stress-map.org>.

Htwe, Y. M. M. & WenBin, 2008: S. Gutenberg-Richter Recurrence Law to Seismicity Analysis of Southern Segment of the Sagaing Fault and Its Associate Components. at <http://174.122.150.229/~gripwebo/gripweb/sites/default/files/Gutenberg-Richter%20Recurrence%20Law.pdf>

Johnson, D., and Dudgeon, 1993, Array signal processing: Prentice Hall.

Kratz, M., Aulia, A. , & Hill, A., 2012: Identifying Fault Activation in Shale Reservoirs Using Microseismic Monitoring during Hydraulic Stimulation: Source Mechanisms, b Values, and Energy Release Rates at <http://www.cseg.ca/publications/recorder/2012/06jun/Jun2012-Identifying_Fault_Activation_in_Shale.pdf>

Maxwell, S., 2010, Microseismic: Growth born from success: The Leading Edge, **29**, 338–343, doi:10.1190/1.3353732.

Maxwell, S. & Chen, Z., 2012: Microseismic Monitoring of Ball Drops During a Sliding Sleeve Frac at <http://www.cspg.org/documents/Conventions/Archives/Annual/2012/085_GC2012_Microseismic_Monitoring_of_Ball_Drops.pdf>

Meehan, D. N., 2010, Completion techniques in shale reservoirs at <http://blogs.bakerhughes.com/reservoir/2010/09/18/completion-techniques-in-shale-reservoirs/>

Neyman, J., and E. Pearson, 1933, On the problem of the most efficient tests of statistical hypotheses: Philosophical Transactions of the Royal Society of London, **231**, no. 694–706, 289–337, doi:10.1098/rsta.1933.0009.

Reshetnikov A., Kummerow J., Buske S., and Shapiro, S.A., 2010: Microseismic imaging from a single geophone: KTB. *SEG Expanded Abstracts* 29, 2070, DOI:10.1190/1.3513252

Shemeta J. and P. Anderson, 2010: It's a matter of size: Magnitude and moment estimates for microseismic data. *The Leading Edge*, **29**, pp. 296 – 302. Doi 10.1190/1.3353726

Taylor, N., Snelling, P., Hwang, K., Stacey, M., Abott, & D. (2012). *Horn River Microseismic Acquisition: Designing a Shallow Array.* GeoConvention 2012. Calgary, Canada.

Warpinski N., (2010): The physics of surface microseismic monitoring. Pinnacle Fracture Diagnostics Tech Update, H07119 05/10. http://www.pinntech.com/pubs/TU/TU10_MS.pdf , accessed October 26, 2010.

Williams-Stroud, S. C. & Eisner, L., 2011: Stimulated Fractured Reservoir DFN Models Calibrated with Microseismic Source Mechanisms, ARMA 10-520

The Cordova Embayment, 2012 at < http://northof56.com/oil-gas/article/the-cordova-embayment>

McPhail, S., Walsh, W., Lee, C., 2008: Shale units of the Horn River Formation, Horn River Basin and Cordova Embayment Northeastern British Columbia at ttp://www.empr.gov.bc.ca/Mining/Geoscience/PublicationsCatalogue/OilGas/OpenFiles/Documents/PetroleumGeology/PGOF2008-1.pdf>

Zhang, Y., Eisner, L., Barker, W., Mueller, M., & Smith, K. (2011). *Consistent imaging of hydraulic fracture treatments from permanent arrays using a calibrated velocity model.* EAGE Third Passive Seismic Workshop – Actively Passive! Athens, Greece: EAGE.

Zhebel, O., D. Gajewski, and C. Venelle, 2010: 80th Annual International Meeting, SEG, Expanded Abstracts, 29, 2181–2185, doi:10.1190/1.3513278.

UNCONVENTIONAL RESOURCES TECHNOLOGY CONFERENCE
FUELED BY SPE • AAPG • SEG

2015 COPYRIGHT FORM FOR URTeC

Thank you for presenting at the Unconventional Resources Technology Conference (URTeC). We appreciate your willingness to present your paper. URTeC's Policy is to safeguard contributed works by obtaining copyright in the name of URTeC. Therefore, a transfer or assignment of copyright is required.

Copyright assignment protects reproduction and distribution of the paper. URTeC shall control the use and may offer to sell and/or collect royalties for use of the paper. However, URTeC permits authors and their employers to retain certain rights to make copies and reuse the material. The author/employer also retains all interest in the proprietary material disclosed in the paper.

For and in consideration of the potential publication of the manuscript or extended abstract (the Work) submitted, I, the submitter of the Work, as Author or for and on behalf of all authors and/or owners of copyright in the Work (Authors), hereby agree to transfer, assign, and convey all right, title, interest, and copyright in the Work and the right to publish the Work in online (including wirelessly conveyed), removable media, and/or printed form to the three societies, Society of Petroleum Engineers (SPE), American Association of Petroleum Geologists (AAPG), and the Society of Exploration Geophysicists (SEG) that make up URTeC effective when the Work is submitted for presentation at the 2015 Unconventional Resources Technology Conference and related publication, subject only to limitation expressed in this Transfer of Copyright.

I warrant and represent that I am empowered and authorized to represent Authors with respect to this Transfer of Copyright if this group includes others besides me. Authors warrant that they are empowered to convey the publication right described above to URTeC and that the Work does not infringe any copyright or invade any right of privacy or publicity. Authors further warrant that they have secured permission for the use of materials from a copyrighted source and all illustrations and photographs used in the Work. Authors agree to indemnify, defend, and hold URTeC, its directors, officers, employees, and agents harmless against any claims to the contrary. Authors understand and agree that URTeC may, at any time, republish in any form the whole Work or parts thereof in any future publication with SPE, AAPG, and SEG at the discretion of URTeC. Authors convey to URTeC non-exclusive right to license distribution or republication of all or any portion of the Work to third parties. Authors retain all other rights. Authors confirm that the Work has not been published previously, nor is it under consideration by any other publisher. This transfer of Copyright shall be binding on Authors' heirs, executors and administrators.

Authors' Royalty-free Rights

Authors of Works published in conjunction with URTeC shall retain the following royalty-free rights:

1. The right to reproduce the Work, including figures, drawings, tables, and abstracts of the Work, with proper copyright acknowledgment, for any purpose.
2. All proprietary rights in the Work that were not transferred to URTeC, including the right to any patentable subject matter that might not be contained in the Work.
3. The right to make oral presentation of the same or similar information as that contained in the Work, provided proper acknowledgment is made of URTeC copyright ownership and current publication status.
4. The right to post the Work or portions thereof on Authors' own Web pages or on Web pages or institutional repositories operated by authors' employers, in either case with acknowledgment of URTeC copyright and a link to an official version published online by URTeC. If Authors' online posting or reproduction of the Work in another form constitutes a modification of the Work as published by URTeC, an accompanying notification stating this is required.

URTeC Control ID Number 2455932

Title of Paper DEVELOPMENT OF UNIFIED DFN USING SURFACE MS EVENT DETECTION

Authors (Name all) CLAUDIO VIRUES, JASON HENDRICK, SUDHENDU KASHIKAR

Author/Authorized Agent Name (Please Print) CLAUDIO VIRUES

(Author/Authorized Agent Signature) | Date JUNE 1st, 2016

United States Government Certification

This will certify that all authors of the paper are U.S. government employees and prepared the paper within the scope of their official duties. As such, the paper is not subject to U.S. copyright protection.

(Author/Authorized Signature) Date

Crown Copyright Certification

This will certify that all authors of the paper are employees of the British or British Commonwealth government and prepared the paper in connection with their official duties. As such, the paper is subject to Crown Copyright and is not assigned to URTeC. The undersigned acknowledges, however, that URTeC has the right to publish, distribute and reproduce the paper in all forms and media.

(Author/Authorized Signature) Date